A geophysical correlation between near-surface radioactivity and subsurface faults detected by gravity method for a region located in the western desert of Iraq

Wadhah Mahmood Shakir AL-Khafaji*[1], Hayder Abdul Zahra Al-Dabbagh[2]

1. University of Baghdad, College of Science for Women, Department of Physics, Iraq
2. Ministry of Science and Technology, Department of Geophysics, Iraq

Abstract

This research study deals with the processing and interpretation of the total Bouguer anomaly and the total count iso-radiation data for a region located in the western desert of Iraq. The research aims to delineate the approximate locations and the effective depth of faults and how does rocks radioactivity act nearby the faults. The graphical method adopted to separate the residual fields from regional's, in order to be processed later by applying the horizontal gradient filter. The results displayed as maps and profile section which delineate qualitatively the approximate locations of faults and quantitatively the high radio counts and major faults effective depth within the region. The results of this study showed that the major faults within the region extend with the directions NW-SE, with effective fault depth ranges of 1.7 – 4.9 Km. High radiometric anomalies detected near or between fault locations as they detected after conducting a gravity-radiometric profile section across the region. Peaks of high radiation total counts are located over the elevated blocks which produced by faulting action. The detected faults penetrate the main groundwater aquifer in the region and this considered responsible for transporting radioactive elements to the surface over and nearby the detected fault locations to form spots of accumulated radioactive deposits.

Keywords: Faulting Gravimetry, Faulting Radioactivity, W- Desert Iraq

1. Introduction

For a long period of time, the gravity method was applied to detect subsurface rock body's geometry and its mass distribution. Such method has its vital importance in the comprehension of subsurface geological structures which are very helpful for subsurface detection goals. The gravity method is very helpful to be applied to faults, cavities, and buried channels detection. The gravimetric anomaly is very useful in conducting location, shape, depth of the subsurface structures (Toushmalani 2010; Biswas 2015). Gravity method widely applied to detect the deep crustal rocks and near-surface mineral ores and provides a clear vision about the rocks density subsurface distribution and subsurface structures. Most of the rocks have some significant traces of radioactive elements with variable rates. Therefore, a radiometric survey was successfully applied to detect radioactive ore bodies. Researchers explained rocks radioactivity on the basis of uranium and thorium disintegration which produce trace radioactivity. Later, researchers showed that K40 isotope is also radioactive, although it forms 0.021% only of crustal rocks, it may contribute in increasing rocks radioactivity due to the expanding dispersion within the crustal rocks. Geophysicists basically used to detect regions which have high and abnormal ɤ-ray records, excluding α and β rays which are detectable only for few centimeters above the ground level

----
*Corresponding author.
E-mail address (es): wadhahmk@yahoo.com

(Sharma 1986). Aero-radiometric survey and total count mapping has its important role in detecting natural radiometric background and to delineate the radioactivity of some exposed to surface sedimentary rocks. Such rocks are mostly belongs to Quaternary and cover some parts of the western desert of Iraq. Furthermore, this method is helpful in studying the structural and geological processes which are responsible of increasing the radiometric intensity at some locations within the surveyed area (Al-Dabbagh 2005).

Al-Nahab and Hanafi (1978) concluded that sediments around springs in some locations at the western desert contain anomalous concentrations of radiometric elements which have been transported from high depths of groundwater aquifers to the surface in a form of water springs produced by faulting. The centers of high radiometric anomalies are located over and nearby the water spring locations as it mentioned by Al-Marsoumi (1982). Springs along the Euphrates River are characterized by higher radioactive concentrations as compared with other locations (Al-Atia and Mahdi 2005; Mahdi and Al-Timimi 2009; Al-Bassam et al. 2013). They explained that groundwater discharges from Euphrates Formation aquifer which has relatively high uranium concentrations in its upper part and represents the main groundwater aquifer in the region as the following: when groundwater seeps at surface in a form of springs they appear at surface as pounds, when they dry by evaporation in a sequent manner the

uranium concentration increases accumulatively. Livinson (1980) and Al-Bassam et al. (2013) mentioned that when U^{+4} get oxidized to U^{+6} to become highly transportable in aqueous systems in the form of uranyl ions.

Faults and other structural features in the current study region is shown by the modified tectonic map of Iraq (Sissakian et al. 1996), which compared later with the residual Bouguer map and total count residual iso-rad map of the region. The airborne radiometric geophysical survey was performed by the French General Company of Geophysics (C.G.G.) under supervision of the Iraqi Geological Surveying and mining company (GEOSURV). Bouguer Gravity data in this research represents a ground geophysical survey performed by (GEOSURV) and published as a map by AL-Kadhimi and Fattah (1994) which covers the whole region of Iraq, in this research only the concerned part to the current study region was processed and interpreted. Gravity field qualitative and quantitative interpretation for the residual gravity anomalies has been adopted by (AL-Khafaji 2014-2017) to detect the approximate fault locations and effective depth estimation for some regions in Iraq. The latter method is applied in the current research with the assistance of iso-rad data interpretation.

Generally, the radioactive background of metamorphosed sediments is higher than those of igneous and metamorphic rocks with the exception of K-rich granite Telford et al. (1976). During a geophysical aero-radiometric survey, ray particles of α and β are undetectable, especially if the radioactive deposit is covered with a considerable thickness of overburden. Therefore, powerful ɤ-ray radiation which emitted from uranium-series $^{214}_{82}$ Pb and $^{214}_{83}$Bi, considered the most detectable radiation. Radioactive material traces are present in most of igneous and sedimentary rocks. Furthermore, radioactivity occurs in oceanic deposits, oil, and river or spring deposits and in humus and peat (Parasnis 1982).

2. Geological Setting

The study area located near the Saudi Arabia boarders and composes about 12000 Km^2, particularly to the south of Hamir seasonal valley at the western desert of Iraq which bounded by the coordinates $31^000`00"$-$31^044`00"$ N, $41^033`00"$- $42^054`00"$ E (Fig1). According to the modified geological map of (Jassim et al. 1990), which shown in Figure 2, the region shows the following rock formations:

Dugmah - Hartha - Tayarat Formation: Dugmah and Tayarat represent an ideal deposition environment of phosphate rocks, it interfere with Hartha Formation which consists of organic detrital limestone with shale. They belong to upper Cretaceous and appear as small deep blue colored spots at the west of region as shown in Figure 2.
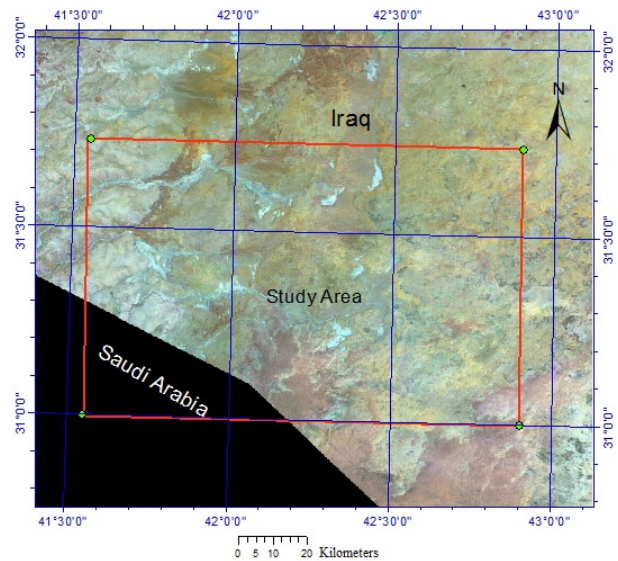
Fig 1. The location of the study region.

Akkashat-Umrdhima Formation: it is composed of detrital limestone, dolomite and dolomitic limestone which belong to Paleocene. Its upper part is composed of chert and phosphate rocks and appears in red color as shown in Figure 2.
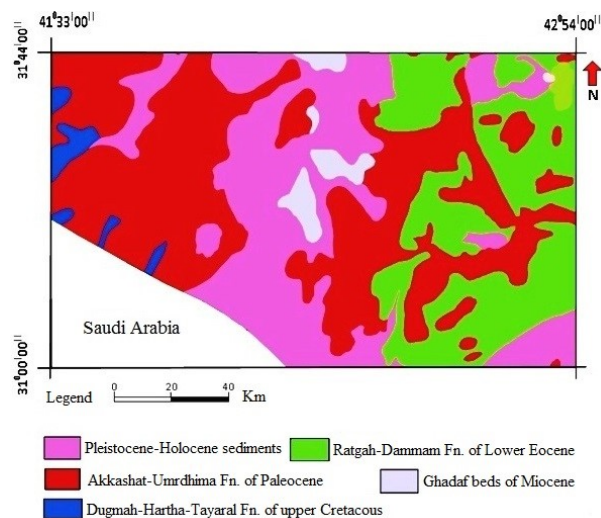
Fig 2. A geological map of the study area showing the exposed to surface geological formations (Jassim et al.1990) modified.

Ratgah-Dammam Formation: it is mainly consists of chalky-organic-detrital limestone of lower Eocene and appears in green color in the geological map of Figure 2. Ghadaf beds of carbonate rocks which belong to the upper and middle Miocene and appear in light blue color in Figure 2.

Quaternary (Pleistocene-Holocene) sediments: regions at the desert plane are covered by top sediments which belong to Quaternary, which sometimes called valley bottom fillings. Such types of sediments were formed during flood periods. Areas covered by this type of sediments appear in pink color as shown in Figure 2.

A part of geological section which published by (Jassim and Goff 2006) is passing near the study area where the stratigraphic sequence could be observed as it shown in Figure 3. According to map of Figure 4, the study region includes two basic structural subzones which are Ubaiyidh and Ma'aniya. They appear in yellow and pink colors in Figure 4. This map shows some important structural features like faults and folds which are found by processing geophysical magnetic and gravity data of previous studies. Some of these features exist within the sedimentary cover and others may extend to the depth of basement rocks as it mentioned by the reference. The map shows that faults in the region extend in three main directions which are NW-SE, N-S and NW-SE.
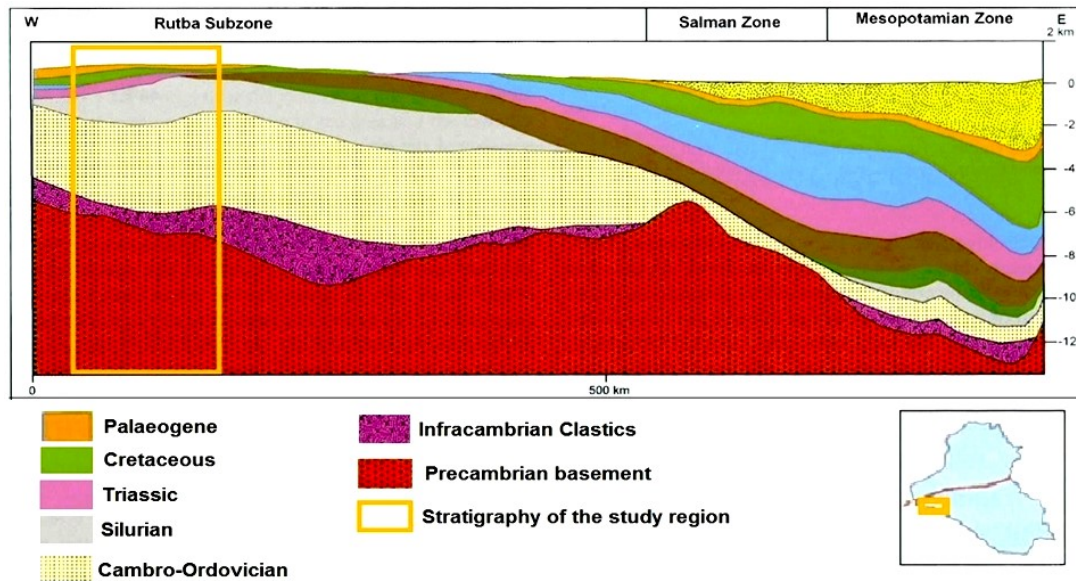
Fig 3. A geological section showing the stratigraphic column of the study area (Modified by: Jassim and Goff 2006)

A reference hydrogeological map of Iraq by (Araim et al. 1990) observed to investigate the depth of groundwater in the study region. According to this reference map, the depth to the groundwater table in the region is about 200m below ground surface. Mostly, the groundwater is rich with sulfate and bicarbonate. Major faults in the region as it proved later in this research extends too much higher depths and may reach to the basement rocks. This means that these faults are penetrating deep across the groundwater aquifer, and therefore springs occur if the water table elevates above ground surface during flood seasons. Spring and well locations in the region is shown in the map of Figure 5.
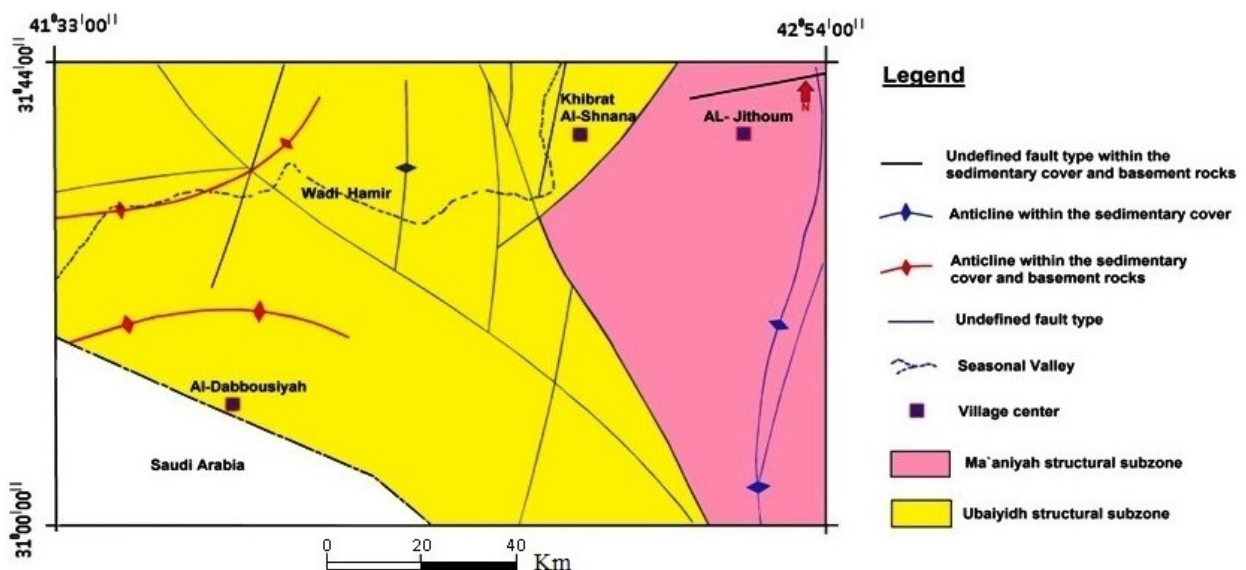
Fig 4. Tectonic map of the study region showing the major structural features in the region (Modified by Sissakian et al. 1996).

Geologically, uranium considered the most important element as its decomposition series covers a greater number of long life. Uranium also associated with alluvial sedimentary rocks like conglomerate and sandstone. Furthermore, uranium exists with phosphate deposits of Akkashat region in the western desert of Iraq (AL-Sanawi 1982).

The Seismologic map of Figure 6 represents an earthquake catalogue and showing that the current study area location does not show any active seismicity. This map was conducted for the period between 1900 and 2009, by compiling all available information about the tectonic setting in the region including the active faults terms of moment magnitude (Mw), Onur et al. (2016).
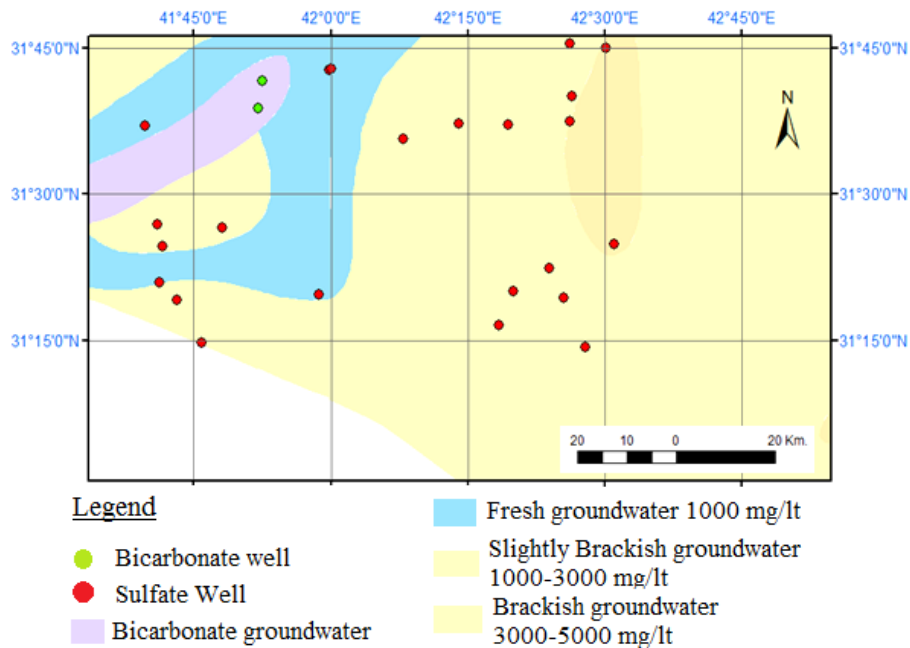
Fig 5. A map showing the spring and well locations and groundwater types in the region, (Modified by Araim et al. 1990).
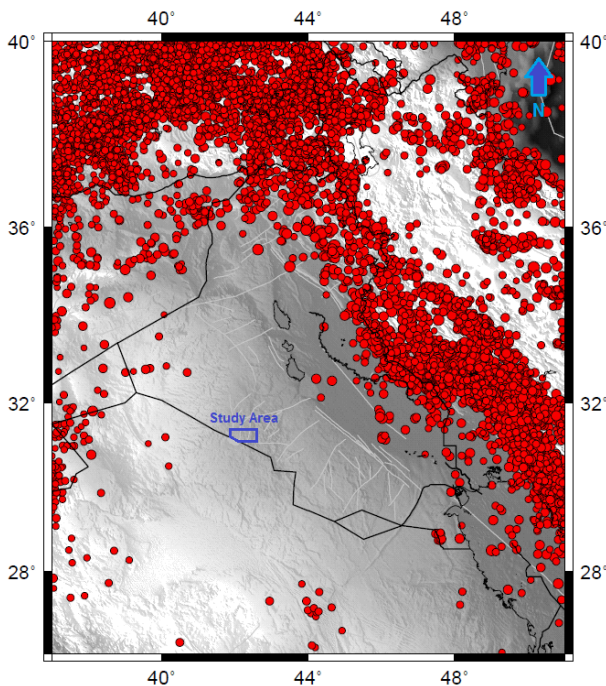
Fig 6. A map which represents the instrumental seismicity Catalogue in Iraq in terms of moment magnitude (Mw) where Mw > 3, Onur et al. (2016).

3. Material and Methods
3.1. Geophysical Data
Total Bouguer anomaly map of Iraq by (AL-Kadhimi and Fattah (1994) was prepared according to gravity ground surveying. The only concerned part to the study region was used to conduct the digital gravity grid of the current research. The process includes the increasing of contour density for the original map, then gridding it with a pattern of $10Km^2$ before input to computer software.

The airborne radiometric survey of Iraq was achieved by the French company CGG in 1974, and the results of the survey presented as a radioactivity map with the scale of 1:200000. This map represents the natural radiometric activity for the elements K, U and Th. The flight lines elevation for this survey was 140 m above the ground surface with the spacing of 2Km between flight line and other in the direction $N30^0E$, and other connecting flight lines with a spacing of 10 Km in the direction $N60^0W$. The instrument used in this survey was the Gamma-Ray Spectrometer it consists of 800 inch^3 NaI thallium activated crystal with four recording channels: K^{40} (K) with recording range (1.35-1.57 MeV) and characteristic peak at 1.46 MeV; Bi^{214} (U) with recording range (1.63-1.89 MeV) and characteristic peak at 1.76 MeV; TI^{208} (Th) with recording range (2.42-2.82 MeV) and characteristic peak at 2.62 MeV; and the total count has

the range of (0.24 – 3 MeV). The total count iso-rad map visualizes the radioactivity for different exposed to surface geological rock units by measuring ɤ-ray emissions which belong to relatively higher depths especially when faults, fractures, and joints exist (Al-Dabbagh 2005).

3.2. Methods

In this research study two geophysical methods adopted which are: the iso-radiation map processing and the total Bouguer anomaly map processing and interpretation. The aim was to locate the major faults in the region and how does radioactive anomalies differentiate according to these faulting locations, then discussing the results according to the geological point of view.

3.2.1. Bouguer gravity anomaly map processing

After constructing the digital Bouguer anomaly map,(Fig 7), a graphical method applied to construct the residual anomaly from the total. The regional gravity field map constructed by the application of the 2nd order polynomial regression. By subtracting the regional gravity grid data values from those of the Bouguer field, the residual gravity grid data was obtained and used to draw the residual gravity map of (Fig 8).
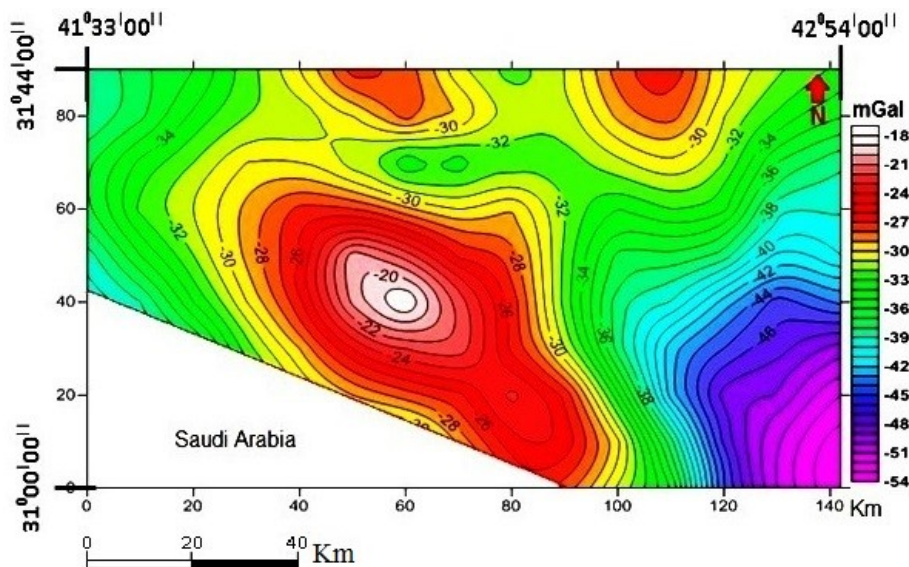
Fig 7. The Bouguer anomaly map, C.I. =1 mGal

The residual gravity anomaly map reflects the density variation within the sedimentary cover over the basement rocks. Major sudden variations in the residual gravity appear in the locations where contour lines value change its value abruptly from low to high values. Therefore we could consider zero value contour lines are the possible locations of faults in the region, especially that some faults like (F2) location in the residual Bouguer map of Figure.8, agrees with the fault location in previous structural map of Figure 4.

Primarily, possible fault locations could be assigned by the residual gravity map (Fig 8), but it is still not so clear how does the gravity field vary with distance. Therefore, the horizontal gradient filter applied on the residual field in order to construct another indicative map like the one which appear in Figure.9. Such map could give more precise locations for the major faults in the region and the maximum contour values would refer to the positions of faulting inflection points within the residual gravity anomaly.

It was proposed to draw a section along the profile line A-A´ which appears in the figures 8, 9 and 10, the gravimetric parameters in addition to total radiation counts, are all displayed in the section of Figure.11.

From this section, we could observe that the positive peaks of filtered data curve are referring to the four locations of the detected faults. In other words, the gradient positive peaks refer to the inflection points of the residual anomaly. Four possible fault lines have been detected F1, F2, F3 and F4 which are trending in the direction NW-SE, as it shown in the Figure 9.
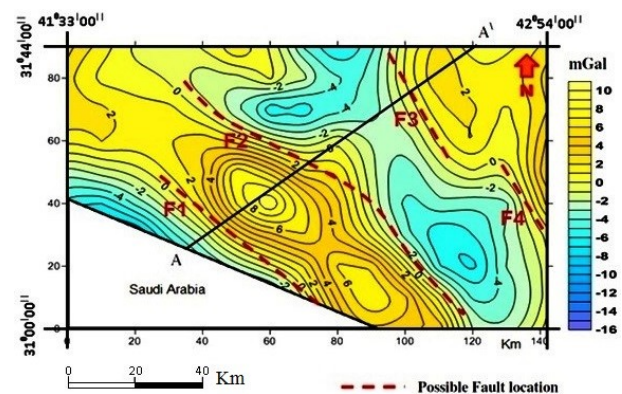
Fig 8. The residual Bouguer gravity map. The trend of extracted basement possible fault is NW-SE, C.I. =1 mGal
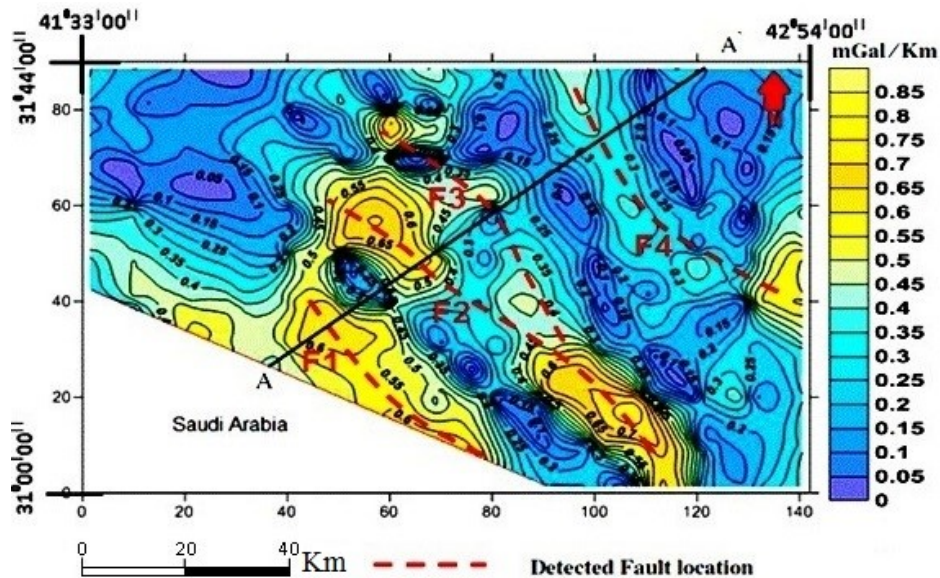
Fig 9. The horizontal gradient filter applied on the residual Bouguer gravity map. The trend of the extracted basement possible faults is NW-SE, C.I. =0.05 mGal/Km

The inflection point represents the midpoint where the residual anomaly changes its mode from minimum to maximum and considered as the fault plane location (Toushmalani 2010). Basically the positive part of gravity anomaly is produced by a dense slab which has a thickness of (t) hosted by less density rocks. The density difference between the dense slab and host rocks is expressed as the density contrast ($\Delta\rho$). Furthermore, the horizontal distance when anomaly changes its mode from $1/2$ Δg_{max} to $1/4$ or $3/4$ Δg_{max} on the profile distance axis is considered as (z), which represents the depth to the center of the dense slab. The distance between the observation point at anomaly minima to inflection point is expressed as (x), Figure 11-a. Therefore, Δg around a fault could be expressed by the equation (Sharma 1986; Dobrin 1976):

(G $\Delta\rho t$) ϕ or $\Delta g = 2Gt\Delta\rho(\pi/2 - \tan^{-1} x/z)$

Where: ϕ is the solid angle which subtends the slab at the observation point which is usually located at anomaly's minimal, G is the gravity constant. The depth to the center of the dense slab (z) could be expressed as the faulting effective depth in this research study. Figure 11-b shows how (z) is variable across the profile A-A'.This depth variation mainly produced by faulting action which makes some rock blocks get elevated and others to lower down. The density contrast ($\Delta\rho$) of the current region rocks is considered to be about (0.95 Kg\m^3), it reflects the density contrast between the dense limestone slab of 2.75 Kg/ m3, and the hosting rocks of perforated limestone with evaporates which has a density of 1.8 Kg\m^3. Further information about different rock densities could be found in (Parasnis 1971; Sharma 1986).

3.2.2. Total count Iso-rad map processing

One of the most effective types of radiation detectors is the scintillation counter. Such instrument consists of a special thallium activated crystal which scintillates as it absorbs ɤ-ray, then, a photocathode inside a tube of photomultiplier amplify pulses to get recorded (Parasnis 1982).

The instrument special crystal has the property of limiting light when struck by ɤ-ray, and each ray generates a tiny spark in the crystal. The photomultiplier tube is a very sensitive electric eye which converts the light impulses into electric impulses. It works to multiply the original voltage to deliver amplified pulses of electricity for every flash of light. Pulses could be recorded by a rate meter or output as audio signals similarly to that of Geiger counter (AL-Sanawi 1982). The radiation intensity recorded as count per minute or milliroentgen per hour. There are some factors which control the instrument reading like scattering and absorption of radiation in earth rocks, irregularity of topography, and the radioactive elements dispersion produced by weathering. Thus, aero-radiometric measurements give possible results to map lithology and lithological contacts for a surveyed region. This has been concluded from the possibility of detecting K, U and Th concentrations from aero-surveys (Parasnis 1982).

The results of an aero-radiometric survey which used in the current research presented finally as total count iso-rad contour map. Such map represented the natural radioactivity for (K, U, Th) elements.

Iso-rad contour map describes the locations of high and low radiometric anomalies in the region. The interpretation also depends on the local geology and

topography. Radiometric surveys indicate areas where radioactive elements are present. Some geophysical investigations described radiometric anomaly according to its circular shape or what called (halo-Phenomena), which indicate the presence of oil deposits in the range of contact between gas and water. Radioactive anomalies may provide good information about the nature and physical properties of rocks. Therefore, such surveys may be used to locate lithological contacts and faults as indicated by increasing intensity of ɤ-ray which may produce by radon gas migration through faults and fracture planes (AL-Sanawi 1982).
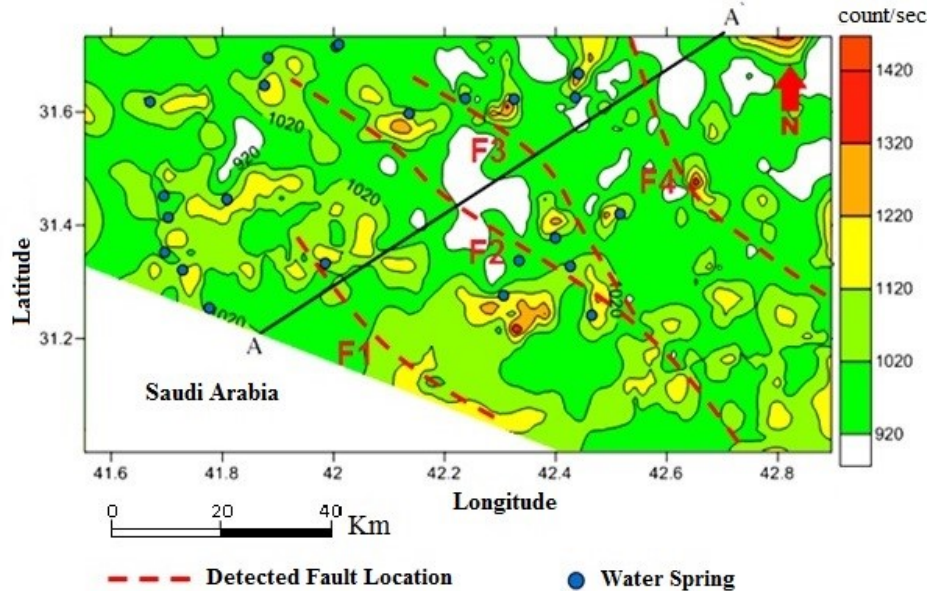
Fig 10. The airborne total count iso-radiation map showing the extracted basement possible faults locations which obtained from the residual gravity field, C.I. =100 count\Sec.

In the current research, a suitable gridding prepared for the iso-radiation map and input to a computer software to get transformed in to a digital contour map like the one of Figure 10. This map shows the locations were radioactivity becomes high and low according to region geology which also affected by the structural situation of the region. Subsurface detected faults by using gravity method were superimposed on the iso-radiation map as shown in Figure 10. By observing this map, it could be noticed that high radioactive anomalies are located between and over fault lines.

4. Results and Discussion
Fault line locations have been assigned by the horizontal gradient filtering for the residual gravity anomaly as shown in Figure 9. Later, a cross section along the traverse line A-A` was very useful in interpreting the gravimetric and radiometric fields qualitatively and quantitatively as it shown in Figure 11. Gravimetric parameters in addition to total radiometric counts are plotted at the same section along the profile line A-A`, Figure 11. This figure represents a model which conducted to show the gravimetric-radiometric variation according to the effective faulting depth across the region. The residual gravity anomaly and its horizontal gradient were applied successfully to detect the locations of the major faults across the study region. The quantitative interpretation of the residual gravity anomaly was used to find the effective depths of major faults. The depth to the center of faults was ranging between 1.7 to 4.9 Km. The dense slab which produced the positive gravity anomaly was about 0.34 Km in thickness, as shown in the model of Figure 11-B.

Table 1, display some readings obtained from the gravity – radiometric section along the profile A-A` as it shown in figure 11. The gravity horizontal gradient positive peaks, (Figure 11-A), are obviously located over the residual anomaly inflection points. This has been considered as the key to locate the major fault plane locations across the region. Generally, radiation total counts rise in some locations where the dense slab become closer to the surface or shallower in depth as shown in Figure 11-A., when the radioactivity counts curve rise to record 1020 – 1040 counts∕sec.

Table 1. Some readings obtained from the gravity- radiometric section of figure 11.

Detected Fault No.	Gravity horizontal gradient value (mgal\Km)	Total radiation counts at the fault location (count\sec.)	Depth to the center of the effective dens slab (Km)
F1	0.7	1020	3.3
F2	0.64	960	1.7
F3	0.46	920	2.5
F4	0.37	1005	4.9
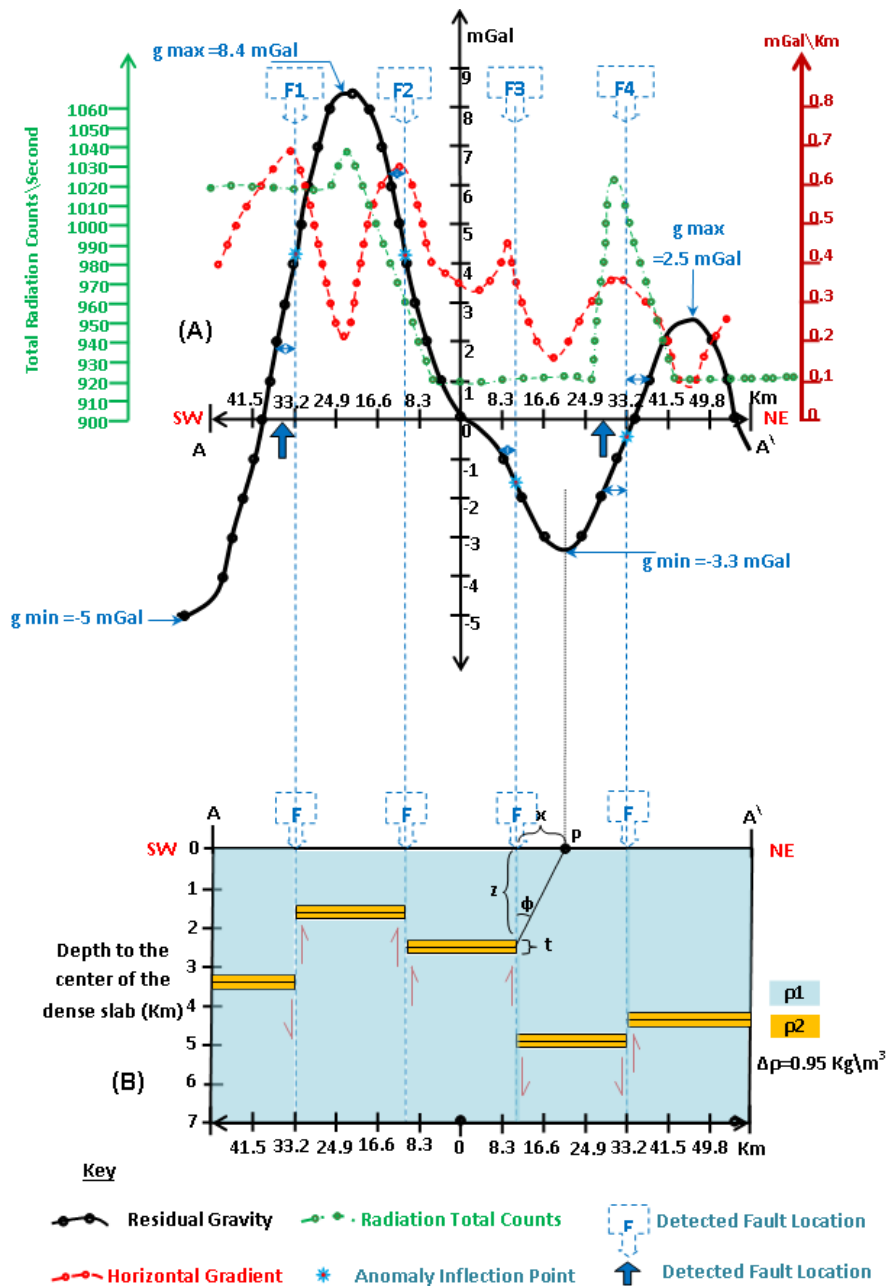
Fig 11. (A): Gravity – Radiometric parameters variation section along the profile line A-A` which its location appears in the figures 8, 9 and 10.   (B): The effective depth of faults according to the dense slab principle.

5. Conclusions

The gravity field interpretation visualized four major faults in the region which extend in the direction NW-SE. Gravity horizontal gradient application was effective in detecting the location and extension of faults. The radioactivity map showed that high radioactive anomalies are generally located on the faulting sides and over faulting planes. The main reason behind this feature is that faults allow groundwater to seep in a form of water springs at the surface and transfer radioactive materials from high depths to surface. Such materials deposit near or between faulting plane areas in an accumulative manner with time. Major faults penetrate to high depths which exceed the groundwater aquifer in the region and their effect may continue to the depth of basement rocks. Rising basement blocks may make the underground radioactive source to become relatively shallower and this has been reflected as high total radioactivity counts. The faults may let the radioactive radon gas to escape from high depths to surface at the faulting plane locations and this explains the rare high radioactive anomalies over some faulting locations.

Recommendations

It is recommended to increase the geophysical data at the faulted areas like achieving a seismic refraction geophysical surveying in order to provide more evidences about the subsurface faults in the region.

References

AL Sanawi S (1982) Introduction to Applied Geophysics, 1st Ed., Printed by the University of Baghdad- Iraq, 144 pages.

Al-Atia M, Mahdi M (2005) Origin and Mode of Formation of Abu Skhair uranium deposits, middle Iraq, *Iraqi Bulletin of Geological Mining* 1:15-27 (in Arabic).

Al-Bassam KS, Beni TJ, Ameen GF, Al-Basrawi NH, Raheem AS (2013) Environmental Geochemical and Radiometric Survey in the Vicinity of Abu Skhair Uranium Mine, Najaf, Iraq, *Iraqi Bulletin Of Geology and Mining* 9:131-149.

Al-Dabbagh HA (2005) Qualitative Interpretation of Regional Radiometric Airborne Survey for Gaara-Higher Euphrates Region (West of Iraq), Ph.D. Dissertation, University of Baghdad, College of Science, Department of Geology, 142 pp.

AL-Kadhimi JAM, Fattah AS (1994) Bouguer Anomalies map of Iraq, published by Iraqi GEOSURV, Baghdad /Iraq.

AL-Khafaji WMS (2014) A Geophysical Study to Evaluate the Groundwater Reserve and Structural Situation of South Sinjar Anticline Region NW-Iraq, Ph.D. Dissertation, University of Baghdad, College of Science, Department of Geology, 171 pages.

AL-Khafaji WMS (2016) Gravity field interpretation for subsurface faults detection in a region located SW-Iraq, *Iraqi Journal of Science* 57:2270-2279.

AL-Khafaji WMS (2017) Gravity Field Interpretation for Major Fault Depth Detection in a Region Located SW- Qa'im / Iraq, *Baghdad Science Journal* 14:625-636.

Al-Marsoumi AH (1982) Geochemical Detection of radioactive Materials Accumulation at Heet- shithatha region, Ph.D. Dissertation, University of Baghdad, College of Science, (unpublished).

Al-Nahab M, Hanafi A (1978) a Ground spectrometric survey at Shithatha, State Department of Geological Survey and Mining, Laboratory Report No. 929, 21 pages.

Araim HI, Al-Wasity JA, Al-Ani SS (1990) Hydrogeological Map of Iraq, scale 1:1000000, published and printed by S.E. of Geological Survey and Mineral Investigation, Baghdad-Iraq.

Biswas A (2015) Interpretation of residual gravity anomaly caused by simple shaped Bodies using very fast simulated annealing global optimization, *Geoscience Frontiers* 6: 875–893.

Dobrin MB (1976) Introduction to Geophysical Prospecting, Mc Graw Hill Inc.,747 pages.

Jassim SZ, Hagobian DH, Al-Hashimi HA (1990) Geological Map of Iraq, scale 1:1000000, Iraqi GEOSURV, Baghdad-Iraq.

Jassim SZ, Goff JC (2006) Geology of Iraq, Dolin, Prague and Monrovian museum, Brno.341pages.

Levinson A (1980) Introduction to Geochemical Exploration, 3rd edit., Applied Publishing Ltd., Calgary, 12 pp.

Mahdi M, Al-Tamimi M (2009) Preliminary evaluation of the uranium contaminant level in the groundwater of the Iraqi Southern and Western Deserts, *Iraqi Bulletin Of Geology and Mining* 5:21-28, (in Arabic).

Onur T, Gok R, Abdulnaby W, Shakir AM, Mahdi H, Numan NMS, Al-Shukri H, Ghlaib HK, Ameen TH, Abd NA (2016) Probabilistic seismic hazard assessment for Iraq, *LLNL Technical report*, 20 pp.

Parasnis DS (1971) Physical Property Guide for Rocks and Minerals, ABEM, Stockholm. *Geophysics Memorandum* 4171, 12 pp.

Parasnis DS (1982) Principles of Applied Geophysics, 3rd Ed., published in the USA by Chapman and Hall, 275 pp.

Sharma PV (1986) A Geophysical Methods in Geology, 2nd Ed., Elsevier Science Publishing Company Incorporation, 442 pages.

Sissakian VK, Al-Kadhimi JAM, Diekman DB, Fattah AS (1996) Tectonic map of Iraq, scale 1:1000000, sheet No.2, 2nd Ed., National Library Legal Deposit No.10, Baghdad-Iraq.

Telford WM, Geldart LP, Sheriff RE, Keys RE (1976) Applied Geophysics, Cambridge University Press.

Toushmalani R (2010) Application of Gravity Method in Fault Path Detection, Australian, *Journal of Basic and Applied Sciences* 4: 6450-6460.